1

What Drives the Central Velocity Dispersion in Nearby Early-Type Galaxies?

GIJS A. VERDOES KLEIJN (ESO), ROELAND P. VAN DER MAREL (STScI),
JACOB NOEL-STORR (COLUMBIA/STScI)

Abstract

The majority of nearby early-type galaxies contains detectable amounts of emission-line gas at their centers. The emission-line ratios and gas kinematics potentially form a valuable diagnostic of the nuclear activity and gravitational potential well. The observed central gas velocity dispersion often exceeds the stellar velocity dispersion. This could be due to either the gravitational potential of a black hole or turbulent shocks in the gas. Here we try to discriminate between these two scenarios.

1.1 Introduction

Optical emission-line gas is detected in at least 50% of the centers of nearby early-type (E/S0) galaxies (e.g., Phillips et al., 1986; Goudfrooij et al., 1994; Macchetto et al., 1996; Ho et al., 1997). The gas velocity dispersion $\sigma_{\rm gas}$ (corrected for instrumental broadening) typically increases towards the nucleus, reaching values similar to the the central $\sigma_{\rm star}$ as measured through 100s of pc scale sized apertures (e.g., Zeilinger et al., 1996). Closer to the nucleus, $\sigma_{\rm gas}$ often exceeds $\sigma_{\rm star}$ (e.g., Ferrarese et al., 1996; Macchetto et al., 1997; van der Marel & van den Bosch 1998; Cappellari et al., 2002; Verdoes Kleijn et al., 2002). Potential contributors to $\sigma_{\rm gas}$ are motions due to (i) a black hole (BH) gravitational potential or (ii) shocks/turbulence in the gas. In the former case, $\sigma_{\rm gas}$ could be caused by three dimensional motion of collisionless cloudlets of gas. More likely, the collisional gas is expected to have settled in a disk. In that case, $\sigma_{\rm gas}$ will be caused by differential rotation over the aperture. However, shocks and/or turbulence can contribute to $\sigma_{\rm gas}$ if there is a permanent input of kinetic energy (perhaps the active galactic nucleus) to sustain them. Thus, determining the driver of $\sigma_{\rm gas}$ has implications for measurements of the BH mass ($M_{\rm BH}$) and the flow properties of potential BH accretion material. Here we present preliminary modeling of $\sigma_{\rm gas}$ and $\sigma_{\rm star}$ in the nuclei of 16 active and 4 quiescent early-type galaxies to constrain the relative importance of gravitation and shocks/turbulence.

1.2 Sample and Data

The galaxy sample consists of 16 active galaxies with radio-jets taken from the UGC FR I sample (see Noel-Storr et al., these proceedings, for selection criteria) and four relatively quiescent early-type galaxies (NGC 3078, NGC 4526, NGC 6861 and IC 1459) (Table 1). The four quiescent early-type galaxies were selected to have

Table 1.1. *Early-Type Galaxy Sample.*

Galaxy (1)	Type (2)	$M_{\rm B}$ (3)	D (Mpc) (4)	Galaxy (1)	Type (2)	$M_{\rm B}$ (3)	D (Mpc) (4)
NGC 315	E+:	-21.9	67.9	M87	E+0-1 pec	-21.4	15.4
NGC 383	SA0-:	-21.4	65.2	NGC 5127	E pec	-20.6	64.4
NGC 541	cD	-21.2	73.3	NGC 5490	E	-21.1	69.2
NGC 741	E0:	-21.9	70.2	NGC 7052	E	-19.9	55.4
3C 66B	E	-21.1	84.8	3C 449	S0-:	-19.6	68.3
NGC 2329	S0-:	-21.1	76.7	NGC 7626	E pec:	-21.1	46.6
3C 264	E	-21.0	84.4	NGC 3078	E2-3	-20.6	35.2
UGC 7115	E	-20.4	90.5	NGC 4526	SAB(s)0	-20.5	16.9
NGC 4335	E	-20.3	61.5	NGC 6861	SA(s)0-:	-20.2	28.1
M84	E1	-20.8	15.4	IC 1459	E3	-21.1	29.2

The galaxies are taken from the UGC FR I radio galaxy sample (Noel-Storr et al., these proceedings) except for NGC 3078, NGC4526, NGC 6861 and IC 1459. Col.(2): Hubble classification from NED. Col.(3): Absolute blue magnitude from LEDA. Col.(4): Distances from Faber et al. (1989), Tonry et al. (2001), or, if not available, directly from recession velocity and $H_0 = 75 \mathrm{kms}^{-1}\mathrm{Mpc}^{-1}$. Col.(5): Galaxy is part of the UGC FR I sample (1) or not (0).

central dust and/or gas disks. Four of the 21 UGC FR I galaxies were not included here because either $\sigma_{\rm star}$ is not available or the location of the nucleus could not be determined reliably, mainly due to dust obscuration

HST/STIS (HST/FOS for IC 1459) emission-line spectra are available for the sample. They include the Hα+[NII] and [SII]6716,6731 lines. A central $\sigma_{\rm gas}$ per galaxy is determined by fitting single Gaussians to each of the lines in Hα+[NII] and [SII]6716,6731 at the nucleus. An analytic emission-line flux profile is determined by fitting a double exponential to the emission-line surface brightness measurements from the HST/STIS spectra and HST/WFPC2 emission-line images (where available). The central stellar dispersion $\sigma_{\rm star}$ for the sample galaxies was obtained from the LEDA catalog*.

1.3 Collisionless Gas Models

Can the gravitational potential of a BH mass induce gas motions which explain $\sigma_{\rm gas}$? Current observations are consistent (e.g., Kormendy & Gebhardt, 2000, for a review) with most (and perhaps all) early-type galaxies containing a black hole with a mass related to $\sigma_{\rm star}$, i.e., the '$M_{\rm BH} - \sigma_{\rm star}$' relation (Gebhardt et al., 2000; Ferrarese & Merritt, 2000). We compute the expected $\sigma_{\rm gas}$ for such a BH mass under idealized circumstances. We assume the gas is a collisionless isotropic spherical distribution of gas cloudlets orbiting the BH. The predicted gas velocity

* LEDA database can be found at `http://leda.univ-lyon1.fr`

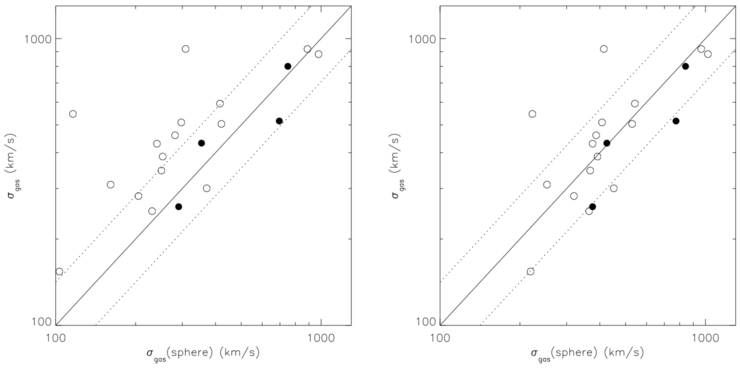

Fig. 1.1. The observed gas velocity dispersion $\sigma_{\rm gas}$ as a function of predicted velocity dispersions for radio galaxies (open circles) and relatively quiescent galaxies (filled circles). (a): The model for $\sigma_{\rm gas}$(sphere,1) assumes an isotropic spherical distribution of gas cloudlets orbiting a BH with a mass according to the $M_{\rm BH} - \sigma_{\rm star}$ relation. (b): similar to (a) but now including the stellar mass distribution as well. The dashed and solid lines indicate $\sigma_{\rm gas}$(sphere)= $(1\sqrt{1/2}, 1, \sqrt{2}) \times \sigma_{\rm gas}$ respectively (to facilitate comparison to the $M_{\rm BH} - \sigma_{\rm star}$). The figure suggests the gas might be largely collisionless: see text for details.

dispersion $\sigma_{\rm gas}$(sphere,1) takes into account aperture size, PSF and instrumental line width.

Fig. 1.1a shows that $\sigma_{\rm gas}$ typically exceeds $\sigma_{\rm gas}$(sphere,1). However, the calculation neglects the stellar mass present, which will increase $\sigma_{\rm gas}$(sphere,1). To illustrate the possible effect of this, Fig. 1.1b shows $\sigma_{\rm gas}$(sphere,2) assuming an isothermal spherical stellar mass distribution in addition to the BH mass, i.e., $\sigma^2_{\rm gas}(\rm sphere, 2) = \sigma^2_{\rm gas}(\rm sphere, 1) + \sigma^2_{\rm star}$. $\sigma^2_{\rm gas}$ typically agrees within a factor 2 to $\sigma^2_{\rm gas}$(sphere,2). In other words, the $M_{\rm BH}$ needed to account for $\sigma^2_{\rm gas}$ agrees within a factor $\sim$ 2 with $M_{\rm BH}$ as predicted by the $M_{\rm BH} - \sigma_{\rm star}$ relation (because $M_{\rm BH} \sim \sigma^2_{\rm gas}$), under these simplifying assumptions. The estimated intrinsic scatter in the relation is also a factor 2 (Tremaine et al., 2002). Thus, an additional contribution to $\sigma_{\rm gas}$ from collisions (e.g., shocks/turbulence) is not required in this case.

Alternatively, we can assume that the collisional gas settles in a disk. We idealize the disk as an infinitely flat disk of gas particles/cloudlets, inclined by 60° to the line

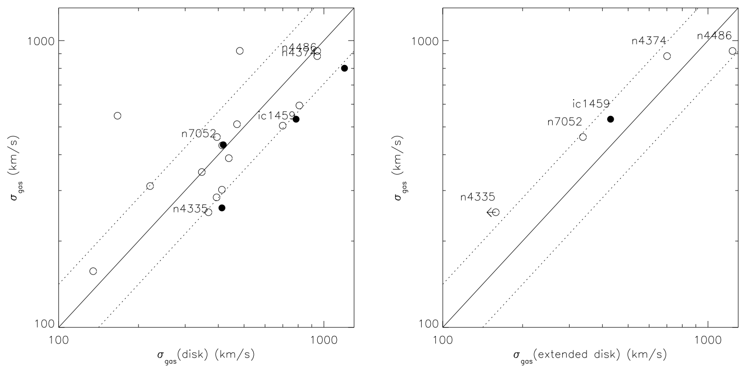

Fig. 1.2. The observed gas velocity dispersion $\sigma_{\rm gas}$ as a function of predicted velocity dispersions for radio galaxies (open circles) and relatively quiescent galaxies (filled circles). (a): The model assumes an infinitely thin gas disk in circular rotation, inclined by 60° to the line of sight and a BH mass $M_{\rm BH}$ according to the $M_{\rm BH} - \sigma_{\rm star}$ relation. (b): same as (a), but now for $M_{\rm BH}$ inferred from published, detailed modeling of the gas mean velocities $v_{\rm gas}$. The figure suggests that $v_{\rm gas}$ and $\sigma_{\rm gas}$ cannot be simultaneously fit by the gas disk model: see text for further details.

of sight, and in circular rotation in the same combined BH and stellar potential as used in the spherical case. On the nucleus, the differential rotation will broaden the emission-line flux profile. Fig. 1.2a shows that the predicted gas velocity dispersion $\sigma_{\rm gas}$(disk) roughly agrees with $\sigma_{\rm gas}$. Hence no shocks/turbulence are required on average; a similar result as for the gas spherical model.

Gas dynamical models of galactic nuclei, based on gas mean velocity $v_{\rm gas}$ instead of $\sigma_{\rm gas}$ often reach a different conclusion. For five sample galaxies, the central BH mass has been measured directly from gas mean velocities $v_{\rm gas}$ in extended gas disks. Fig. 1.2b shows that the velocity dispersion $\sigma_{\rm gas}(v_{\rm gas})$ predicted by our gas disk model for *these* BH masses underpredicts $\sigma_{\rm gas}$ in four cases. Hence, an additional contributor to the velocity dispersion is needed to explain the observed values in our gas disk model. This agrees with the mean velocity modeling which invokes an additional source of dispersion, 'gas turbulence', to explain $\sigma_{\rm gas}$ (Maciejewski & Binney, 2001; van der Marel & van den Bosch, 1998; Cappellari et al., 2002; Verdoes Kleijn et al., 2002). Only for NGC 4486 does a detailed gas disk modeling by

Macchetto et al. (1997) account for both $v_{\rm gas}$ and $\sigma_{\rm gas}$, consistent with our modeling. It is reassuring that our simplistic modeling is consistent with the more detailed gas dynamical models on the difference between NGC 4486 and the other four galaxies.

It is less reassuring that Fig. 1.2b suggests that a thin, circular gas disk model in general cannot explain simultaneously observed gas velocities and dispersions. For a simultaneous fit one has to invoke gas turbulence. Alternatively, the extended gas might somehow rotate at subcircular velocities, which would lead the models to infer a lower BH mass and hence lower nuclear differential rotation.

Qualitatively, Fig. 1.1 suggests another possible solution to this problem: the gas changes from a flat disk configuration outside the nucleus to a (more) spherical distribution closer to the nucleus. The nuclear spherical gas distribution explains the central $\sigma_{\rm gas}$. Furthermore, the new configuration implies that (i) the flat gas disk effectively has an inner radius and (ii) only part of the observed nuclear emission-line flux is coming from a disk. Both changes put the gas associated with the circular disk at a larger mean distance from the BH, compared to the continous disk model, and hence at lower circular velocities for the same BH mass.

1.4 Discussion & Conclusions

The simple models discussed above suggest that the observed excess in velocity dispersion in nuclear emission-line gas disks could be explained by a more spherical gas distribution towards the nucleus. In such a model, the gas remains collisionless (as in the customary single gas disk model) and thus avoids invoking ad hoc turbulence or shocks which require a permanent input of kinetic energy to persist. Nevertheless, it could well be that activity associated with the BH can provide such a continuous input of energy. The outliers in Figs. 1.1 & 1.2 and the tendency for the collisionless models to underpredict $\sigma_{\rm gas}$ more for active galaxies rather than for quiescent galaxies perhaps favor this scenario.

More sophisticated modeling and further observations can help to determine between different gas configurations. On the one hand, more accurate modeling of the stellar mass density and the emission-line velocity profiles are expected to decrease the predicted $\sigma_{\rm gas}$ at fixed BH mass. The central density profile of bright ellipticals is generally shallower than an isothermal distribution. Emission-lines often show extended wings: the true 2nd moment is then larger than the Gaussian 2nd moment. This effect is taken into account in the gas disk model, but not in the spherical model. On the other hand, emission-line flux profiles are typically marginally resolved. They may contain a significant contribution from an unresolved component which can be arbitrarily close to the BH. This might increase the predicted $\sigma_{\rm gas}$.

UV spectroscopy can determine directly if shocks are present. In the presence of shocks the gas can be shock-ionized. If absent, the emission-line gas is only photoionized. The two ionization mechanisms produce different UV emission-line ratios (e.g., Dopita et al., 1997).

In summary, the current results cannot distinguish between the various gas configurations. However, accurate BH mass measurements (and hence BH demography) and BH accretion models depend on such a distinction. Improvement of the simplistic gas dynamical modeling presented here and UV observations can help to resolve this.

References

Cappellari M., et al., 2002, ApJ, 578, 787
Dopita M.A., et al., 1997, ApJ, 490, 202
Faber S.M., et al., 1989, ApJS, 69, 763
Ferrarese L.C., Ford H.C., Jaffe W., 1996, ApJ, 470, 444
Ferrarese L.C., Merritt D., 2000, ApJ, 539, L9
Gebhardt K., et al., 2000, ApJ, 539, L13
Goudfrooij P., Hansen L., Jorgensen H.E., Norgaard-Nielsen H.U., 1994 A&AS, 105, 341
Ho, Fillipenko & Sargent, 1997, ApJ, 487, 568
Kormendy J., Gebhardt K., 2002, in The 20th Texas Symposium on Relativistic Astrophysics, eds. H. Martel, J.C. Wheeler, AIP, 363
Macchetto F.D, et al., 1996, A&AS, 120, 463
Macchetto F.D., Marconi A., Axon D.J., Capetti A., Sparks W., Crane P., 1997, ApJ 489, 579
Maciejewski W., Binney J., 2001, MNRAS, 323, 831
Phillips M.M., Jenkins C.R., Dopita M.A., Sadler E.M., Binette L., 1986, AJ, 91, 1062
Tonry, J. L., et al., 2001, ApJ, 546, 681
Tremaine et al., 2002, ApJ, 574, 740
van der Marel R.P., van den Bosch F.C., 1998, AJ, 116, 2220
Verdoes Kleijn G.A., van der Marel R.P., de Zeeuw P.T., Noel- Storr J., Baum S.A., 2002, AJ, 124, 2524
Zeilinger W.W., et al., 1996, A&AS, 120, 257